ULTRAWIDEBAND INDOOR LOCATION AND TRACKING SYSTEM

by

QING CHEN
B.S. University of Central Florida, 2005

A thesis submitted in partial fulfillment of the requirements
for the degree of Master of Science
in the School of Electrical Engineering and Computer Science
in the College of Engineering and Computer Science
at the University of Central Florida
Orlando, Florida

Summer Term
2006

ABSTRACT

The objective of this thesis is to demonstrate an indoor intruder location and tracking system with UltraWideBand (UWB) technology and use data compression and Constant False Alarm Rate (CFAR) techniques to improve the performance of the location system. Reliable and accurate indoor positioning requires a local replacement for GPS systems since satellite signals are not available indoors. UWB systems are particularly suitable for indoor location systems due their inherent capabilities such as low-power, multi-path rejection, and wide bandwidth. In our application, we are using UWB radios as a radar system for tracking targets in indoor locations. We also use Discrete Cosine Transform (DCT) to compress the UWB scan waveforms from the receivers to the main computer to conserve bandwidth. At the main computer, we use Inverse DCT to recover the original signal. The UWB intruder detection system has the indoor tracking accuracy of four inches. There are many military and commercial applications such as tracking firefighters and locating trapped people in earthquake zones, and so on. This thesis demonstrates the capability of a UWB radar system to locate and track an intruder to an accuracy of four inches in an indoor cluttered environment.

ACKNOWLEDGMENTS

I would like to express my deep-felt gratitude to my advisor, Dr. Damla Turgut of the School of Electrical and Computer Science at University of Central Florida for her advice, encouragement, enduring patience, and constant support. She was never ceasing in her belief in me and also constantly driving me with energy to reach my goal on completing this thesis. She has always given me her time, in spite of anything else that was going on. Her comments, suggestions, and advicement were invaluable to the completion of this work.

I also want to thank my committee members, Dr. Joseph Berrios and Dr. Samuel Richie of the School of Electrical Engineering and Computer Science at University of Central Florida for their time, suggestions, comments, and additional guidance to this thesis. As a special note, Ravi Palaniappan at Institute of Simulation and Training graciously volunteered to act as my mentor throughout this thesis. He was extremely helpful in providing the additional guidance and expertise I needed to complete this work.

Additionally, I would like to thank School of EECS at University of Central Florida for granting me Accelerated BSEE to MSEE program scholarship to continue on with my education. This award was one of the main reasons for my return to complete the Masters Degree at University of Central Florida. I also like to thank my family and friends for their support during this thesis work.

TABLE OF CONTENTS

CHAPTER 1

INTRODUCTION

A new emerging radio design standard, the term "UltraWideBand" (UWB) which comes from the fundamental physics, benefits of radios designed to use coherent wide-relative-bandwidth propagation. Unlike conventional wireless systems, which use narrowband modulated carrier waves to transmit information, UWB transmits over a wide band of radio spectrum, using a series of very narrow and low-power pulses. UWB can operate on further distances and faster than any other wireless system and results in simple architectures that can deliver high speed radios. The primary advantages of UWB are high data rates, low cost, and low-power. UWB also provides less interference than narrowband radio designs, while yielding a low probability of detection and excellent multi-path rejection. UWB is capable of being used in a multitude of commercial applications ranging from wireless networks (scalable from low to ultra high speeds) to remote sensing and tracking devices and ground penetrating radars [17].

Some of the requirements for indoor location system include rapid setup time, high accuracy, and error margin of less than 1 feet as we will need to determine which floor or side of the wall a target is located. For this work, we develop UWB software algorithms to accurately locate a target in indoors using a Matlab software tool.

Narrow band radio signals limit the information capacity of radio systems because the amount of information carried out is proportional to the bandwidth. The information content that UWB signals can carry increases substantially due to the wide-band of the signal.

A Defense Advanced Research Projects Agency (DARPA) study panel, the group coined

the term ultrawideband in the 1990s, defined it as a system with a fractional bandwidth greater than 25 percent. Fractional or relative bandwidth is the ratio of signal bandwidth over center frequency. If B is the bandwidth, F_c is the center frequency, and F_h and F_l are the high- and low-frequency cutoffs [13].

$$Bf = \frac{B}{F_c} = \frac{(F_h - F_l)}{\frac{(F_h + F_l)}{2}} \tag{1.1}$$

As a result of UWB's distribution of energy, the spectral density is extremely low. UWB emissions are targeted to be lower than currently allowed for unintentional emitters - for example, less than 500 mV/m at frequencies above 2 GHz measured in a 1 MHz bandwidth at 3m distance (FCC Part 15 rules for unintentional emitters in the US). UWB radios transmit less than 75 nanowatts of power per megahertz of frequency bandwidth. This would be equivalent to an aggregated power of 0.26 mW, in contrast to 30 to 100 mW for 802.11b radios and 1 mW to 1 W for bluetooth radios [4].

Instead of traditional sine waveform transmission in which a carrier signal is used to transmit the information carrying signal, UWB systems use carrier-free pulses that span across a wide spectrum. These very low power pulses are used in the coding technique such as pulse position modulation to transmit the signal over long distances. Pulse Position Modulation (PPM) encodes information by modifying the time interval between pulses [14].

The UWB receiver directly converts the received RF signal into a base-band digital or analog output signal.

Some of the characteristics of UWB waveforms are

- Ultra-short duration pulses that yield Ultra-Wide Bandwidth signals
- Extremely low power

- Excellent rejection to interference from other radio systems

Due to the low power limitations set by the FCC, signals of most Ultra-Wideband impulse radios generally appears as white noise to other radios in operation in these lower spectrums.

1.1 UWB radar system

In our current application, we are using UWB as a radar system for tracking targets in indoor location. Compared to conventional radar systems that use narrow band radio signals, we use the large bandwidth of UWB signals for radar application.

Some of the inherent characteristics of UWB signals are useful when applied for radar systems [19] and they are:

- improved target range measurement accuracy. Since the pulse width is very narrow, the UWB signals give better accuracy and resolution.
- identify target classes and types, because the narrow pulse carries information not only about the target as a whole but also its separate elements.
- reduce multi-path effects in cluttered indoor environment because the scattering cross-section of interference sources is reduced relative to the target scattering cross section.
- the UWB radar signals are immune to interference from external narrow band signals.
- it is difficult to detect the low power UWB signals.

1.2 CFAR technique

The signal return from targets is usually buried in thermal noise and clutter, which refers to any undesired signal echo that is reflected back to the receiver by buildings, clouds, the sea, and so on. Since the noise power is not known at any given location, a fixed threshold

detection scheme cannot be applied to the radar returns in individual range cells. An attractive class of scheme that can be used to overcome the problem of clutter is the CFAR processing scheme which sets the threshold adaptively based on the local information of total noise power. The threshold in a CFAR detector is set on a cell-by-cell basis using estimated noise power by processing a group of reference cells surrounding the cell under investigation [7].

The detection threshold is computed so that the radar receiver maintains a constant predetermined probability of false alarm. From equation (1.2)

$$V_T = \sqrt{[2\Psi^2 ln\left(\frac{1}{P_{fa}}\right)]} \tag{1.2}$$

We can see that if the noise power Ψ is assumed constant, then a fixed threshold V_T can satisfy the above equation. However, this condition is rarely true and the noise power varies. Thus, to maintain a constant probability of false alarm, the threshold value must be continuously updated based on the estimates of the noise variance. The process of continuously changing the threshold to maintain a constant probability of false alarm is called Constant False Alarm Rate (CFAR).

The adaptive CFAR techniques detect a target using geographically separated multiple receivers. When setting up the sensors in different locations, it may not be possible to accurately estimate the noise power at the location and setting a constant fixed threshold might increase the probability of false alarm especially if the threshold is set too low. One way to overcome this would be to set an adaptive threshold for the range bins using CFAR technique. The threshold is set on a cell-by-cell basis using the estimated noise power by processing the cells surrounding the cell under the test [3].

1.3 Data compression techniques

Traditionally, the sensor data from the different receivers must be transmitted to a collection point to determine its usefulness. Intuitively, one understands that it is not efficient to transmit the raw data. There must be compression methods that reduce the needed bandwidth, and yet preserve the accuracy of the sensor data. We plan to investigate data compression techniques such as Discrete Cosine Transforms (DCT) to reduce the bandwidth requirements for the sensor data transmission. DCT utilizes a fixed transform matrix whose basis vectors closely approximate those of the class matrices in which the Karhunen Loeve transform belongs (Principal Component Analysis). Because of the fixed nature of the DCT matrix, it does not adapt well to the input signal, but it is implementable in real-time.

There are two types of DCT techniques: lossy and lossless data compression. Lossy data compression method is the one where compressing data and then decompressing it retrieves data that may not be identical to the original form, but it closely resembles. The advantage of this method is that it can produce a much smaller compressed file than any known lossless method while still meeting the requirements of the application [18].

1.4 Contribution of this thesis

The UWB intruder detection system is useful tracking assets in indoor locations. One of the major drawbacks of GPS systems are that they do not function effectively in enclosed areas such as urban terrain, caves and tunnels [10]. Our proposed UWB location system not only works in indoor locations, but also provides accurate location information. The accuracy of our system is in the order of one feet while GPS gives location in terms of 3m.

There are many military and commercial applications of this indoor location tracking sys-

tem. For instance, special operation personnel could keep track of their units' movements during urban combat operations. When engaging the enemy in close quarters such as in cities, it becomes essential to locate movement of hostile personnel inside buildings before launching operations. The UWB indoor tracking system can also be used to track firefighters and locate trapped people in earthquake zones.

CHAPTER 2

RELATED WORK

We surveyed the existing technology in the area of indoor location and tracking systems using various Radio Frequency techniques. We also identified their advantages and disadvantages [11]. This chapter presents the related work done on sensor detection using CFAR technique, pulse compression, and UWB radar system.

2.1 Indoor Mobile Wireless Location Technologies

This section describes some of the existing wireless location technologies used for indoor sensor networks.

2.1.1 Localization using wireless ethernet

This technology uses COTS routers and Ethernet adaptors that could serve the dual application of data transmission and location information. These include computing devices such as laptops, PDAs equipped with wireless capability, and so on. One of the advantages of this system is the ubiquitous presence of wireless communication devices in offices and homes. The major disadvantage is the lack of coverage in many areas and accuracy issues.

2.1.2 Cricket localization system

This system uses a combination of RF pulses and ultra-sonic devices. The system must install a unit called cricket compass to the mobile device [15] and measure the time difference between the time-of-flight of the ultrasound and the RF signal. Even though this system is highly de-centralized, it requires setting up an infrastructure around the building which

is not desirable.

2.1.3 Active badge system

This system uses Infra-red tags from fixed transmitters to the mobile receivers to determine the location. This mobile device is attached to a hardware unit called badge which it emits a unique IR signal in every 15 seconds [20]. It is placed at the highest position of the wall or ceiling indoor to pick up the IR signal. The signal is then send to a computer on the wired network which it gives the location. The most obvious disadvantage of this system is that it requires a line-of-sight between the devices as well as high density sensor installation in the building to provide the higher accuracy.

2.1.4 RADAR

The RADAR system implements a location service utilizing the information obtained from an already existing RF data network. It uses the RF signal strength as an indicator of the distance between a transmitter and a receiver [1]. One the disadvantage of this technology is its requirement for extensive calibration to accurately locate the mobile unit. This requires the environment to be stable and may not be applicable in crowded places such as offices.

2.1.5 UWB

There have been recent advances in development of UWB radar system for many applications such as UWB Electronically Steerable Arrays (ESA) and Side Looking Synthetic Aperture Arrays (SLSAR) [9]. Ground Penetrating Radar (GPR) is another important area of using UWB radar systems. GPR works much like conventional radar, using pulses of electromagnetic radiation in the microwave band (UHF/VHF frequencies) of the radio spectrum, and reading the reflected signal to detect subsurface structures and objects without drilling, probing or otherwise breaking the ground surface. Applications include locating buried voids/cavities, underground storage tanks, sewers, buried foundations, ancient land-

fills. It can also be used to characterize bedrock, the internal structure of floors/walls, water damage in concrete, and the internal steelwork in concrete [8]. In [6] a low cost, miniature UWB radar has demonstrated the ability to detect suspended wires and other small obstacles at distances exceeding several hundreds of feet using an average output power of less than 10 mW. Originally developed as a high precision UWB radar altimeter for the Navy's Program Executive Office for Unmanned Aerial Vehicles and Cruise Missiles, an improved sensitivity version was recently developed for the Naval Surface Warfare Center.

Our choice of using UWB over narrow band radios for location and tracking is based on the many inherent advantages as given below.

- Wide band signal - the devices we are using operate at a FCC approved center frequency of 4.7 GHz. They use direct sequence pulse position modulation which is a preferable frequency and scheme for indoor applications because losses through obstruction are lower at this frequency.
- High processing gain of UWB systems
- Availability of hardware resources like UWB radios for measurements and testing

2.2 CFAR Techniques

The basic concepts of the CFAR techniques have been described in the previous chapter. Here, we present the CFAR techniques.

2.2.1 Thresholding approach based on test cell statistics

In [3], the author proposed and analyzed a new constant false alarm rate detection argorithm to select CFAR reference samples based on the statistical property of sample in the test cell. The author compared different CFAR algorithms such as the Cell Averaging (CA)-CFAR, Smallest Of (SO)-CFAR, Ordered Statistics (OS)-CFAR, and Greatest

Of (GO)-CFAR to determine which algorithm outperforms the others in different environment. He concluded that Switching (S)-CFAR is designed to operate in an homogeneous environment and multiple targets with clutter transition situation. It has small CFAR loss comparing with other CFAR processor and also it is simple to design and implement due to the fact that it does not require to have sample ordering.

2.2.2 Analysis of CFAR processors in nonhomogeneous background

In [7], the authors determined that CFAR processors are useful to detect radar targets in background. They have considered five different CFAR processing schemes and analyzed their performances in both homogeneous and nonhomogeneous environment. They compared the fixed optimum threshold with the Average Detection Threshold (ADT) of the CFAR processor to get a measure of the overall loss of detection. For the mean-level CFAR detection, it showed serious performance degradation in nonhomogeneous noise background while CA-CFAR and GO-CFAR showed superior results in homogeneous noise background. The GO-CFAR processor in regions of clutter transition is better than any other mean-level CFAR on false alarm rate performance; however, the detection performance in multiple targets environment is poor. The authors also showed that OS-CFAR processor performed well on handling multiple targets, but it lacks effectiveness in preventing false alarms.

2.2.3 Threshold optimization for distributed order-statistic CFAR signal detection

In [2], the authors used OS-CFAR detection system. They used this detection technique in a distributed detection system with dependent observations from sensor to sensor under the assumption of weak signals. They have applied AND and OR fusion rule and found out OR fusion provides better result than the AND fusion rule for false alarm. They also investigated the ability of other CFAR distributed detection schemes to maintain constant

false alarm probability in the reference observations. Their simulation study showed that OS-CFAR schemes provide much better overall performance than CA-CFAR.

2.3 Discrete Cosine Transform

The Discrete Cosine Transform (DCT) is a Fourier-related transform similar to the discrete Fourier Transform (DFT). DCT is used for data compression of different waveforms such as seismic waveforms. Previous results [18] have shown that DCT is useful for compressing and reproducing the waveforms at approximately one-third of the original rate. The DCT, in particular the DCT-II, is often used in signal and image processing, especially for lossy data compression, because of its "energy compaction" property. For our work, we use DCT to compress the UWB scan waveforms from the receivers to the main computer and use Inverse DCT to recover the original signal.

CHAPTER 3

PRELIMINARY ANALYSIS

In this chapter, we describe the basic concepts of decision and estimation. We introduce the target detection technique used in this thesis.

3.1 Error probabilities and decision criteria

The theory used in this work is error probabilities and decision criteria. A binary decision rule is evaluated in terms of the error probabilities. The probability of a first-kind error, α, is defined as in equation (3.1)

$$\alpha = Prob[d = d_1 | s = s_0] = P[d_1 | m_0] \tag{3.1}$$

where α is the probability of deciding for the event m_1 when the event m_0 occurred and hence the signal s_0 was generated.

In a similar way, the probability of a second kind error, β, is defined as in equation (3.2)

$$\beta = Prob[d = d_0 | s = s_1] = P[d_0 | m_1] \tag{3.2}$$

where β is the probability of deciding for the event m_0 when the event m_1 occurred.

In classical mathematical statistics, the symbols H_0 and H_1 are used in place of m_0 and m_1. m_0 event is referred to as the "null hypothesis", H_0, and corresponds to the absence of statistically meaningful differences between the 'samples', i.e. the observation and the 'population'.

3.1.1 Neyman- Pearson NP Criterion

Neyman-Pearson criterion is the rule used to make the decision on the error of the signal. In order to introduce this rule, we need to know the definition of error probabilities α and β used in radar techniques as in equations (3.3) and (3.4):

$$\alpha = P[d_1|m_0] = P_{FA} \tag{3.3}$$

$$\beta = P[d_0|m_1] = 1 - P_D \tag{3.4}$$

where the event m_1 corresponds to the presence of an object to be detected, and the the event m_0 indicates the absence of targets in detection applications.

In order to have a 'good' decision, it is desirable that the 'false alarm probability' $P[d_1|m_0]$ is as low as possible, whilst the 'detection probability' $P[d_1|m_1]$ should be as high as possible. However, when $P[d_1|m_1]$ grows, $P[d_1|m_0]$ generally increase as well. Figure 3.1 shows the decision regions in Neyman-Pearson Criterion [12].

A convenient strategy is to fix one of the two probabilities at a given value, while the other one is optimised. This is precisely the Neyman-Pearson criterion that can be expressed more formally as follows:

Fix $P[d_1|m_0]$ at a given value α_0 and then maximize $P[d_1|m_1]$; i.e. in signal detection terms: fix P_{FA} then maximize P_D.

This rule corresponds to choosing, among all regions Z_1 where $P[d_1|m_0] = \alpha_0$, the one that maximizes $P[d_1|m_1]$. The decision space Z is partitioned into the two regions:

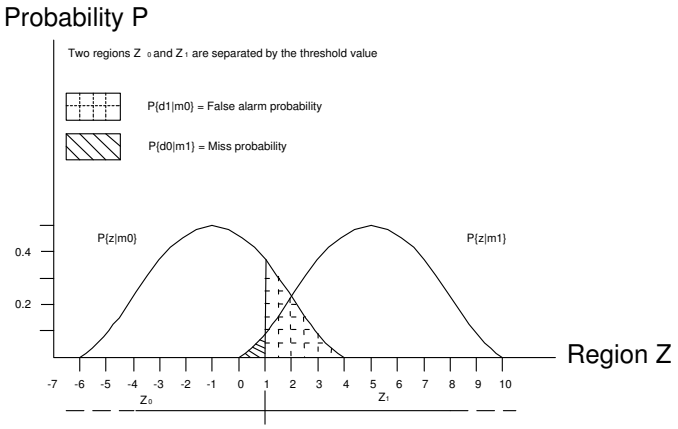

Figure 3.1: The decision regions in Neyman-Pearson Criterion.

$$Z_0 = z : (z) < 1 \tag{3.5}$$

$$Z_1 = z : (z) > 1 \tag{3.6}$$

3.2 Target detection technique

In our UWB radar system, we use a similar technique by fixing the P_{FA} value and determining the probability of detection, false alarm rates and the miss rates.

3.2.1 RF triangulation method for target detection

The primary objective of a location detection system is to accurately locate a target in an environment. There are many techniques for location detection systems such as Angle of Arrival, Direction of Arrival and Time of Arrival methods. In our work,we use the Time of Arrival (ToA) method.

ToA technique is based on the fact the electromagnetic waves travel at a speed of light, an approximately 1 feet per nanosecond. Thus, when a waveform arrives at a receiver from a target reflection after 10 nanoseconds after its transmition, we can estimate that the target is located in a 10 feet from the receiver. But there are two possible locations for the target to be located. We can resolve this by introducing another receiver that eliminates the second possibility and thus enables a 2-dimensional location of the target.

RF triangulation or trilateration is a method of determining the relative positions of objects using the geometry of triangles. To accurately and uniquely determine the relative location of a point on a 2 dimensional plane using trilateration alone, at least 3 reference points are needed in general. Figure 3.2 demonstrates this technique. Let us describe the technique in detail. In simpler terms, with two receivers at known locations, an emitter can be located onto a hyperboloid. Consider a third receiver at a third location. This would provide a second ToA measurement and hence locate the emitter on a second hyperboloid. The intersection of these two hyperboloids describes a curve on which the emitter lies. RF Triangulation is commonly used in civil and military surveillance applications to accurately locate an aircraft, vehicle or stationary emitter by measuring the ToA of a signal from the emitter at three or more receiver sites [16].

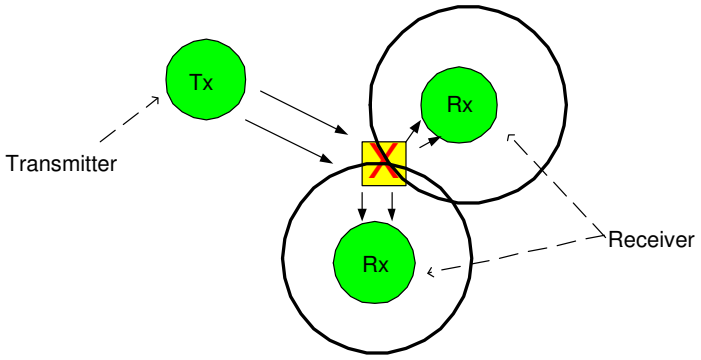

Figure 3.2: Triangulation.

One of the requirements of ToA system is that all the transmitters and receivers have synchronized clocks. This is possible with UWB radios as they transmit clock information in the header packets.

CHAPTER 4

EXPERIMENTAL PROCEDURE

4.1 Hardware and software used

In this chapter, we present the main software and hardware used, data collection, and software design for this thesis. The basic hardware used for this work is UWB wireless transreceiver that emits low-power radio frequency signals. These radios are being developed for home networking and wireless communications market. We chose Matlab as our software tool for the simulation study.

4.1.1 UWB technology

Conventional radar and communication systems use low frequency signal to modulate high frequency carrier waveform, and it is this modulation that contains the information. In UWB technology, this is not the case. There is no carrier frequency, instead, short pulses of energy are emitted. These pulses are of widths of several nanoseconds to 200 picoseconds with resulting bandwidths of several Gigahertz. It is the vast bandwidth that makes for excellent spatial resolution. Our work specifically uses UWB Evaluation Kit (EVK) radios developed by Time Domain Corporation. Figure 4.1 shows the Time Domain P-200 radios used as the intruder detection sensor.

4.1.2 Setup of the P200 EVK radio

In the EVK radio, the duration parameter sets the baseline number of acquisition symbols that are transmitted at the beginning of each packet. The first required step for data

Figure 4.1: Time Domain P-200 radios used as the intruder detection sensor.

reception is called "acquisition". It is responsible for locking the receiver to a transmitter's signal. The system uses a proprietary parallel approach for acquisition to significantly reduce the acquire time. The acquisition portion of the packet contains many different stages of activity and uses a code length of 16 pulses. The first stage of acquisition consists of building a set of ramps and evaluating user specified threshold equations. Once a ramp meets the threshold, the transmitter and receiver are code aligned and roughly frame aligned. The receiver uses the duration parameter to determine how many symbols to search before re-initializing the acquisition process [5].

In order to detect the transmitted signal, a receiver must vary the phase of its sampler circuit across a range of 32768 bins = 104.167 nanoseconds, or one frame. At each phase delay, the receiver dwells for a specified number of pulses and integrates the sampled energy. After each dwell period, the receiver increments the sampler's phase according to the hop size parameter and repeats the process [5]. Figure 4.2 shows the processing of scanning the data in the EVK radio.

The duration should be set equal to the number of symbols needed to scan one complete

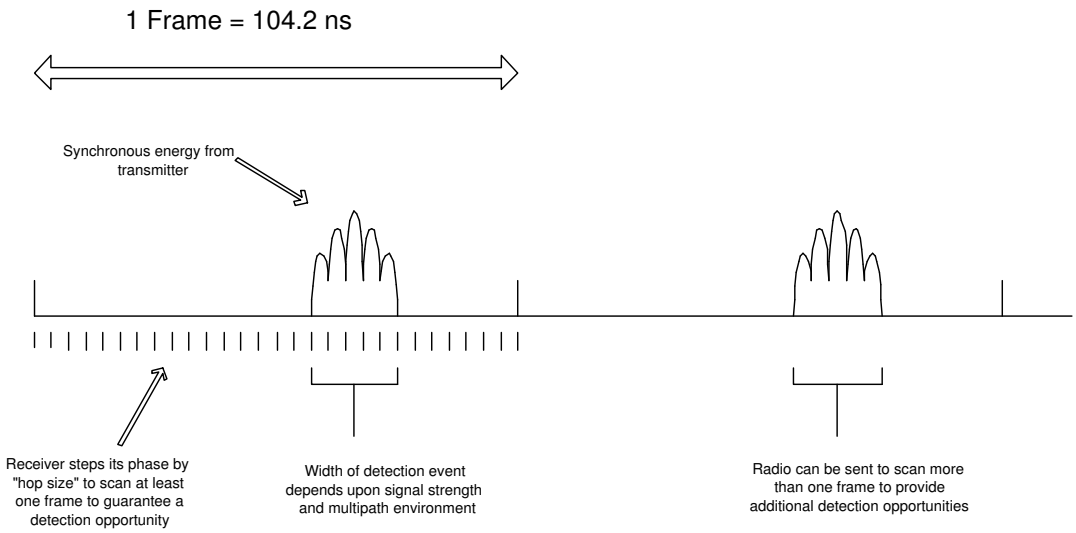

Figure 4.2: Duration setting for scanning the packet in the EVK radio.

frame at the specified hop size. The default hop size for the radio is 82 bins. If we use the formula,

$$Duration = Framesize/HopSize \tag{4.1}$$

the default duration setting is 32768 bins / 82 bins = 399.6 which is approximately 400 symbols. This value should be set equal on both the transmitter and receiver. If the amount is less than 400 symbols, a full frame cannot be scanned fully. As a result, some of the pockets are lost. On the other hand, if the entered amount is more than 400 symbols, more than one frame can be scanned. This leads to possibly increasing the robustness of acquisition at the cost of more acquisition overhead.

In this work, knowing that 32768 bins = 104.167 nanoseconds, we can calculate that one range bins equal to 3.18 picoseconds to transmit the signal. Using the speed of light as $3*10^8$ m/sec, we calculate the distance that the signal travels in 3.17 picoseconds as 0.003128 feet for one range bin.

In transmitting and receiving the packets, we might encounter some packet loss; however, we can prevent loss of packets by increasing the acquisition duration. Before changing the duration, the user should optimize: i) the acquisition threshold constant and ii) acquisition integration. The expected benefit of increasing acquire duration is generally much less than improvements from changing the threshold constant and integration [5].

4.1.3 Ray tracing

Another technique of evaluating PulsON 200 radio wave is by ray tracing. The term "ray tracing" investigates the multiple paths a signal takes to arrive at a receiver. Since the PulsON 200 radio has extreme precise time resolution, we can use ray tracing analysis to correlate time-delayed pulses in the received waveform directly to spatial placement of physical objects in a given environment [5].

For a given transmitter-receiver separation, pulses delayed relative to the first arriving Line of Sight (LoS) pulse can be tied to a range ellipse that corresponds to the time delay. Knowing the speed of light, we can calculate the range ellipse for each time delay. Figure 4.3 shows the calculating the time delays and corresponding range ellipse.

4.2 Data collection

We conducted proof-of-concept experiments to demonstrate the indoor location and tracking capabilities of the UWB system. The UWB radios used for the experiment were Time Domain UWB PulsON trans-receivers operating at a center frequency of 4.7 GHz and a bandwidth of 3.2 GHz. These UWB radios are capable of functioning as communication devices for high speed data transfer between nodes and also as highly accurate radio location devices capable of detecting multi-path signals from targets. For our experiments, we used the UWB radios in bi-static radar mode with the UWB receiver collecting multi-path radar signals from the transmitter and based on the time-of-flight estimating the distance

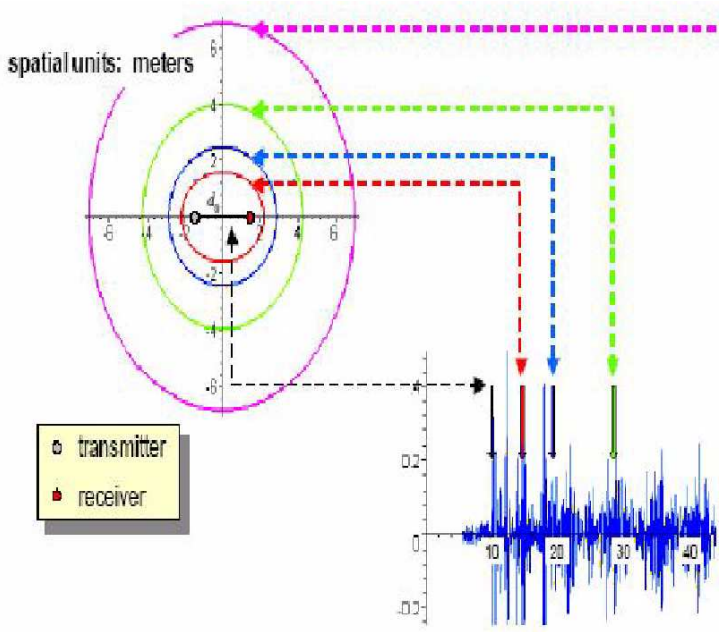

Figure 4.3: Calculating the time delays and corresponding range ellipse.

to targets of interest.

The experiment was setup in Institute for Simulation and Training (IST) conference room with 20 feet distance between the UWB transmitter and the receiver. The UWB radios are capable of ranging among each other to obtain mutual distances between them. We also used a laser range finder to verify the distance between them. We initially measured the background noise signals from the static objects in the room such as tables and chairs. These objects would reflect the UWB transmitted signal which the receiver captures as background clutter multi-path return signals. We measured a set of 10 scans and averaged them to ensure that we have sufficient amount of data for our analysis (see Figure 4.4). This background signal is used to set a "threshold" to detect an intruder.

We then introduced an "intruder" between the transmitter and the receiver (see Figure

Figure 4.4: Experiment setup.

4.5). The intruder was a human subject positioned at the mid-point of the transmitter and the receiver at a distance of 10 feet. We collected multiple intruder data scans and averaged it. This multi-path intruder scans contain a RF signature of the intruder.

We repeated the experiment for distances of 6 feet and 14 feet from the UWB transmitter and collected the multi-path return scans. We then included another receiver on the perpendicular axis and collected multiple intruder scan data. This intruder data is used to locate the intruder position on a 2-dimensional axis (see Figure 4.6).

The scan data collection was achieved using a custom software graphical interface which was developed as part of the software package for using the UWB radios. Our principal work involved using the UWB radios to collect the scan data and developing code in Matlab software for post processing and intruder location.

Figure 4.5: Experiment setup with intruder.

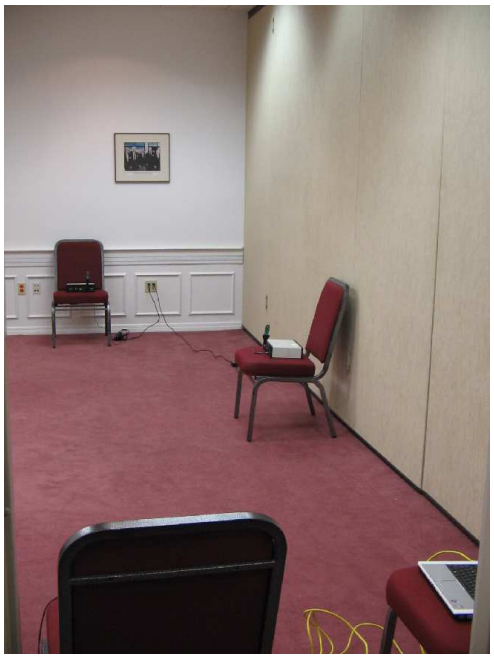

Figure 4.6: Experiment setup with 3 radios.

4.3 Software design

The scans from the experimental procedure were collected on a central computer as data files to be used for post-processing and analysis. The software design for this thesis involved code developing in Matlab software for calculating threshold, CFAR, target detection, and data compression algorithms.

4.3.1 Target detection procedure

The background scans initially collected are averaged over a set of 10 scans to eliminate spurious outliers and glitches due to hardware failures. This background scan data which gives the background clutter noise in the indoor environment is critical in determining the threshold for target detection. We assume that the background clutter is Gaussian noise with mean zero. We validate this assumption in the next section. Based on our assumption we calculate the threshold for the background noise using the relation in equation (1.2).

We use this threshold to determine the number of false alarms for our set of measurements by comparing the background clutter noise to the threshold values for each range bin of the scans. In our case, the false alarm is defined as the number of background scans that exceed the threshold we calculated.

This threshold value serves as a base-line to detect the intruder in the next stage of the software processing. Table 4.1 shows the mean threshold values of all the range bins for increasing values of P_{FA}. As expected, the threshold values decrease for increasing P_{FA}. Based on our calculation of the number of false alarms, we determine that for a P_{FA} of $1e-3$, we obtain a zero probability of false alarm and appropriately set the threshold value for our intruder detection system.

Table 4.1: Mean threshold values for increasing P_{FA}.

P_{FA}	Threshold
$1e{-}10$	131.76
$1e{-}6$	99.662
$1e{-}4$	79.267
$1e{-}3$	67.041
$1e{-}2$	52.48
$1e{-}1$	33.512

4.3.2 CFAR

One of our initial assumptions was that the background noise does not vary over a time period. However, there is a possibility that the background ambient noise can increase due to factors such as furniture or equipment present in the indoor location. This leads to a different multi-path signal to the receivers, a possible variation in the background noise scans, and also affects the threshold parameters we used for our intruder detection. We solve this problem by introducing a CFAR technique which we vary threshold based on the background noise conditions. In our experiments, we vary the threshold value to achieve the lowest number of false alarms. The next stage of our software routine is to determine the presence of the intruder and their location from the intruder scans.

For processing the intruder scans, we average a set of 10 intruder multi-path scans captured over a short period of time to ensure accuracy of the measurements. We then compare the intruder scans to the background noise threshold and determine the range bins at which the intruder scans have exceeded the threshold. This process helps us to calculate the location of the intruder between the transmitter and the receiver. Based on the multi-path radar signature of the intruder, we can calculate the time-of-flight of the bi-static radar signal to

accurately estimate the location of the intruder.

4.3.3 Discrete Cosine Transform

All these processing are performed at a central processing station that collects data from UWB receiver stations which consists of a UWB receiver and a laptop. The sensor data is compressed using Discrete Cosine Transform (DCT) before being sent from the UWB receiver station to the central processor. The data is recovered using inverse DCT at the central processor.

CHAPTER 5

RESULTS

Figure 5.1 illustrates the effect of varying probability of false alarm, P_{FA}, on the threshold level. Using equation (1.2), we calculate the threshold level for each range bin for a specific P_{FA}. For a very low P_{FA} of $1e-10$, the threshold values estimated are high. As we progressively increase the P_{FA} through $1e-6, 1e-4, 1e-3$ and $1e-2$, the threshold decreases. This was illustrated in Table 4.1 in the previous chapter as well. We utilize this plot to emphasize that the probability of false alarm and the threshold are inversely related. A good radar design strives to attain a low probability of false alarm (Type 1 error) to reduce mistakenly triggering the detection system, and also attempts to keep the threshold level low to avoid target misses. A very high threshold might lead to the radar not detecting the target (Type 11 error).

In our intruder detection system, our threshold level for each range bin is calculated from the background noise level measured under ambient noise conditions. Given a specific probability of false alarm, we calculate the threshold for each range bin using equation (1.2). By varying the P_{FA} over a range of values from $1e-10$ to $1e-2$, we calculate the number of false alarms generated which is estimated by comparing the calculated threshold with each background scan. When the background scan exceeds the threshold, we increment the false alarm counter. By trial and error, we estimated the highest value of P_{FA} that does not trigger a false alarm is $1e-3$. Table 5.1 tabulates the number of false alarm for increasing P_{FA}. Table 5.2 shows the probability of detection P_D for increasing P_{FA}.

Figure 5.2 plots a background scan amplitude with the threshold for a series of range bins for P_{FA} of $1e-3$. It can be observed that the background scan levels stay lower than

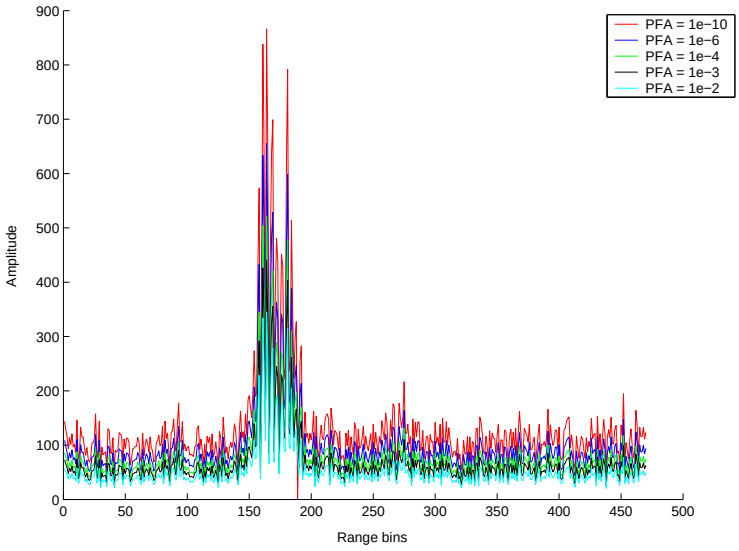

Figure 5.1: Varying P_{FA} on the threshold level.

Table 5.1: Number of false alarm for increasing P_{FA}.

P_{FA}	Number of false alarm
$1e{-}10$	0
$1e{-}6$	0
$1e{-}4$	0
$1e{-}3$	0
$1e{-}2$	1
$1e{-}1$	3

Table 5.2: P_D for different P_{FA}.

P_{FA}	P_D in percentage
$1e{-}10$	20
$1e{-}6$	60
$1e{-}4$	70
$1e{-}3$	80
$1e{-}2$	80
$1e{-}1$	100

the threshold for all the range bins. Let us recall that this P_{FA} generated the optimum threshold level for the lowest number of false alarm. The question may arise, what if we increase the P_{FA} value to $1e-2$? Would the background scans exceed the threshold?

Figure 5.3 provides an answer to this question. This figure shows a magnified part of a background scan and the threshold for a P_{FA} of $1e{-}2$. It can be observed that the threshold is exceeded at range bin 189 to trigger a false alarm signal.

Figure 5.4 shows the background scan range bins exceeding the threshold for a P_{FA} of $1e-1$. This indicates that setting a low threshold causes a large number of false alarms. We have an optimum threshold value for intruder detection with the P_{FA} set to $1e{-}3$. The next stage of our software processing is to subtract the intruder scans from the background clutter noise and compare the resulting scan data to the threshold values. The processing was performed by Matlab code. For our first observation, we plot the intruder scans for the experimental data collected with an intruder at 10 feet from the transmitter.

Figure 5.5 shows the intruder scans with the threshold and the range points at which it exceeds the threshold. From the plot, we observe that the intruder scan crosses the

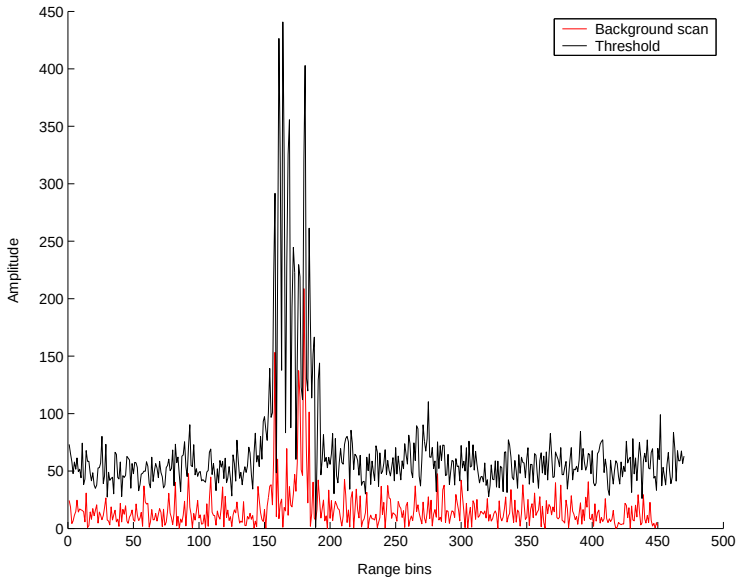

Figure 5.2: Background scan and the threshold for $P_{FA} = 1e-3$.

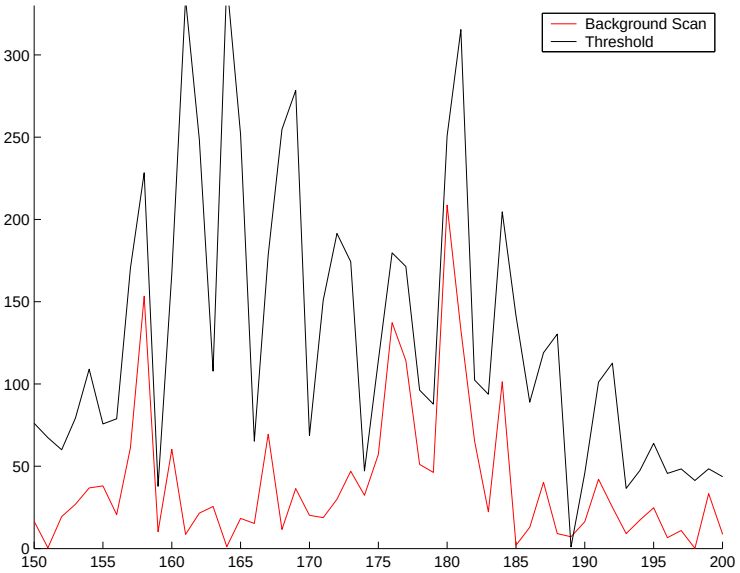

Figure 5.3: Background scan and the threshold for $P_{FA} = 1e-2$.

Figure 5.4: Background scan and the threshold for $P_{FA} = 1e - 1$.

threshold value at the range bin of 313. Using the time-of-flight calculation, we estimate the location of the intruder to be at approximately 10 feet from the transmitter (0.032 * 313) = 10.016 feet. Thus, we have accurately estimated the location of an intruder to an accuracy of inches. To verify our results, we calculated the intruder scans for our measurement values for a 6 feet and plot the results. The intruder scan range bin crossed the threshold at 189 range bin. We convert the range bin to location value of (0.032 * 189) = 6.048 feet which is approximate distance of our intruder from the transmitter. Figure 5.6 shows the range bin that exceeds the threshold for the intruder at 6 feet.

Our results indicate that the intruder could be on either side of the UWB radios as seen in Figure 5.7. We need another set of measurements to validate the position of the intruder. We use another receiver placed on the Y-axis and collect the scan data. This receiver is placed at a distance of 10 feet from the transmitter. The values from the second receiver help to locate the intruder on the 2-dimensional axis as we see from Figure 5.8. From the second receiver scan, we calculate that the range bins exceed the threshold at 6 feet from

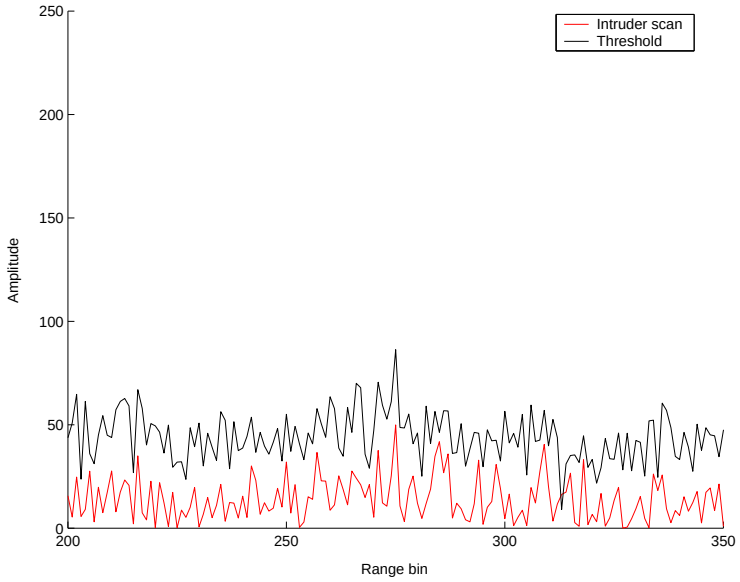

Figure 5.5: Intruder scan at 10 feet.

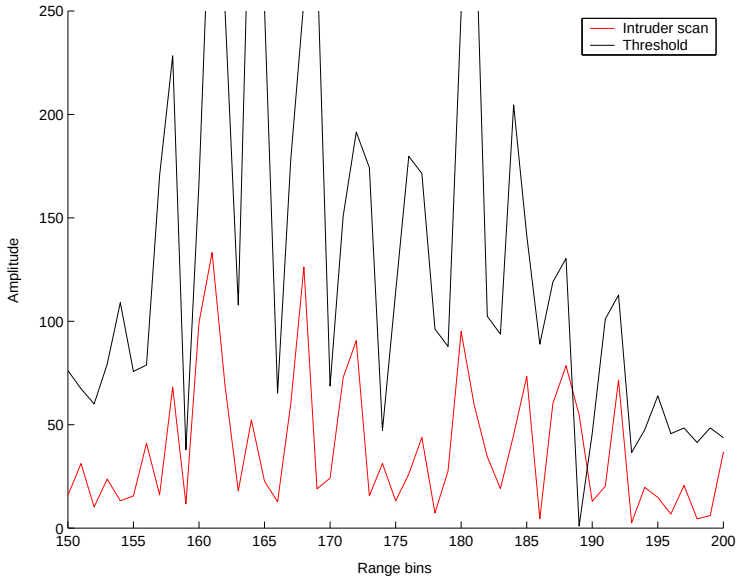

Figure 5.6: Intruder scan at 6 feet.

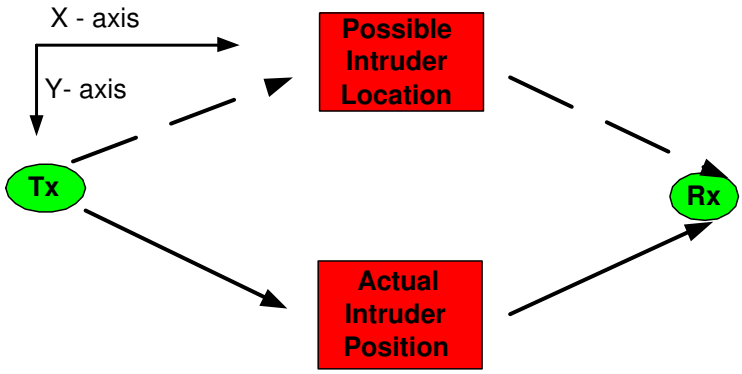

Figure 5.7: 1-dimensional intruder location.

the transmitter as seen from Figure 5.8 for the receiver Ry.

Figure 5.9 plots the original and uncompressed scan waveform stored in the receiver station. Figure 5.10 is the recovered scan waveform using DCT. We can see that the compressed waveform has small oscillations and occupy a smaller bandwidth for transmission. We transmit this compressed waveform to the central processing station that uses Matlab software for post processing.

Thus, by using two 3 UWB radios, we have accurately estimated the location of a single intruder inside a room. This technique can work even if the radios are located outside the confines of the room since UWB radio waves can penetrate the walls.

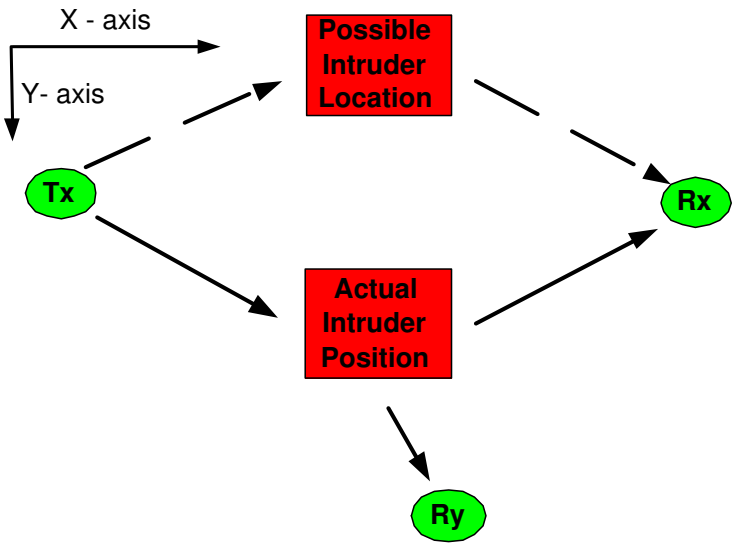

Figure 5.8: 2-dimensional intruder location.

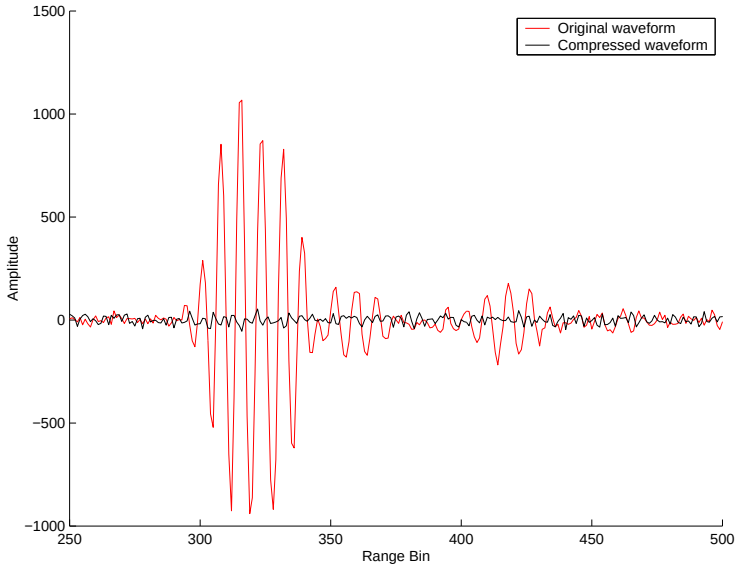

Figure 5.9: Uncompressed and compressed scan waveform.

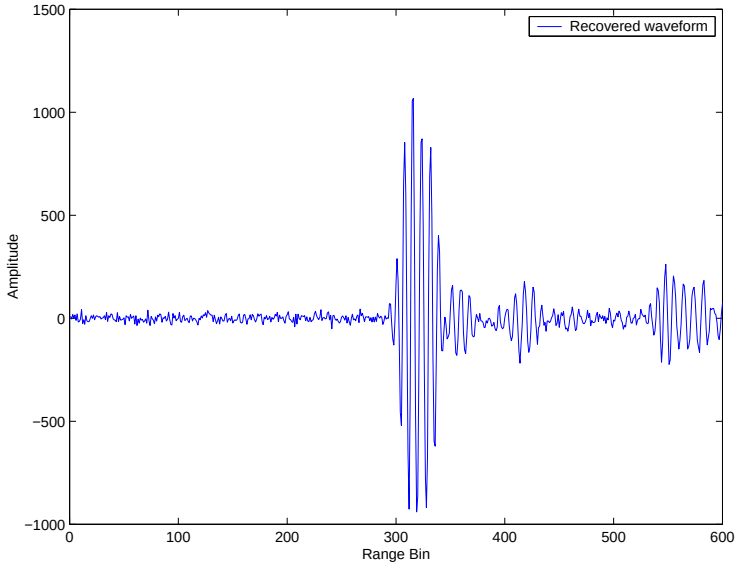

Figure 5.10: Recovered scan waveform.

CHAPTER 6

CONCLUSIONS

Indoor positioning is a demanding application and UWB systems offer a particularly good solution. This project demonstrates a UWB indoor location system that can effectively track an intruder inside a building in 2-dimension. By adjusting the threshold to the varying noise levels in the environment using CFAR and DCT algorithms, we improved the efficiency of the detection system. This work can easily be extended to a 3-dimensional system. Future research can focus on optimizing the algorithm such that it can process scan data at a faster rate and improving the coverage area of the UWB system by using additional number of radios. There are many military and civilian application areas for this location system such as tracking soldiers in urban combat and firefighters in burning buildings.

REFERENCES

[1] P. Bahl. RADAR: An In-Building RF-based User Location and Tracking System. In *Proceedings of the 19th Annual Joint Conference of the IEEE Computer and Communication Societies*, volume 2, pages 26–30, March 2000.

[2] Rick S. Blum and Jinfen Qiao. Threshold Optimization for Distributed Order-Statistic CFAR Signal Detection. volume 32. IEEE Transactions On Aerospace and Electronic Systems.

[3] Tri-Tan Van Cao. A CFAR Thresholding Approach Based on Test Cell Statistics. *Defence Science and Technology Organization (DSTO)*, 2004.

[4] Dajana Cassioli, Moe Z. Win, and Andreas F. Molisch. The Ultra-Wide Bandwidth Indoor Channel: From Statistical Model to Simulations. Technical Report 6, IEEE Journal on Selected Areas in Communications, 2002.

[5] Time Domain Corporation. EVK User's Manual PulsON 200 UWB Evaluation Kit. Technical report, 7057 Old Madison Pike Suite 250, Huntsville, AL 35806 USA, 2001.

[6] R. J. Fontana. An Ultra Wideband Synthetic Vision Sensor for Airbone Wire Detection. Multi-Spectral Solutions, 2001.

[7] P. P. Gandhi and S. A. Kassam. Analysis of CFAR Processors in Nonhomogeneous Background. *IEEE Trans. Aerosp. Electron. Syst.*, 24(4):427–445, July 1988.

[8] Geophysical Survey System Inc. http://www.geophysical.com.

[9] Intelligent Automation Inc. UWB Radar System Development Project. STTR Phase 1 Technical Report, April 2001.

[10] S. J. Ingram, D. Harmer, and M. Quinlan. UltraWideBand Indoor Positioning Systems and Their Use in Emergencies. Technical report, Thales Research and Technology (UK) Ltd., Worton Drive, Reading, RG2 0SB, UK, 2004.

[11] Shomit S. Manapure, Houshang Darabi, Vishal Patel, and Prashant Banerjee. A Comparative Study of Radio Frequency-Based Indoor Location Sensing Systems. In *IEEE International Conference on Networking, Sensing and Control*, pages 1265–1270, March 2004.

[12] James T. McClave, Frank H. Dietrich II, and Terry Sincich. *Statistics*. Prentice Hall, Seventh edition, 1997.

[13] Andreas F. Molisch and Jeffrey R. Foerster. Channel Models for Ultrawideband Personal Area Networks. Technical report, Mitsubishi Electric Research Laboratories, 201 Boardway, Cambridge, Massachusetts 02139, December 2003.

[14] Keveh Pahlavan and Xinrong Li. Indoor Geolocation Science and Technology. pages 112–118, 2002.

[15] N. B. Priyantha, A. K. L. Miu, H. Balakrishnar, and S. Teller. The Cricket Location Support System. In *ACM MOBICOM*, Boston, MA, August 2000.

[16] Loran-C-Us-Navigation-System-for-Marines-and-Coast-Guard. http://www.navcen.uscg.gov/loran/default.htm.

[17] Kazimierz Siwiak. Ultra-Wide Band Radio: Introducing a New Technology. pages 1088–1093, 7057 Old Madison Pike, Huntsville, AL 35806, 2001.

[18] Andreas S. Spanias, Stefan B. Jonsson, and Samuel D. Stearns. Transform Metholds for Seismic Data Compression. *IEEE Transactions On Geoscience and Remote Sensing*, 29(3):407–416, May 1991.

[19] James D. Taylor. *Ultra-Wideband Radar Technology*. CRC Press, First edition, 2001.

[20] R. Want, A Hopper, V. Falcao, and J. Gibbons. The Active Badge Location System. pages 91–102, January 1992.